

SCIENTIFIC REPORTS



OPEN

Human activity accelerating the rapid desertification of the Mu Us Sandy Lands, North China

Yunfa Miao¹, Heling Jin¹ & Jianxin Cui²

Received: 13 November 2015

Accepted: 05 February 2016

Published: 10 March 2016

Over the past several thousand years, arid and semiarid China has experienced a series of asynchronous desertification events in its semiarid sandy and desert regions, but the precise identification of the driving forces of such events has remained elusive. In this paper we identify two rapid desertification events (RDEs) at $\sim 4.6 \pm 0.2$ ka BP and $\sim 3.3 \pm 0.2$ ka BP from the JJ Profile, located in the eastern Mu Us Sandy Lands. These RDEs appear to have occurred immediately following periods marked by persistently frequent and intense fires. We argue that such fire patterns, directly linked to an uncontrolled human use of vegetation as fuel, played a key role in accelerating RDEs by ensuring that the land surface was degraded beyond the threshold required for rapid desertification. This would suggest that the future use of a massive and sustained ecological program of vegetation rehabilitation should reduce the risk of destructive fire.

The arid and semiarid region of North China consists principally of sandy lands, deserts and loess deposits, and lies at the junction of four principal atmospheric circulatory systems (Fig. 1A). Under global warming the risks of desertification and humidification in the sandy areas are carefully evaluated based on the parameters obtained from written records and observational data^{1,2} as well as longer time-series proxies of sedimentary materials (*e.g.*, grain-size^{3–5}, pollen^{6–8} and black carbon⁹ *etc.*), because all of these sources can offer opportunities for understanding the historic relations among desertification, climate and human activities, and thus serve as references for major ecological rehabilitation. More reliable modern research shows that RDEs during the past 10 ka occurred asynchronously in different sandy lands, or even different parts of the same sandy lands^{10,11}; although the driving forces behind these events remain elusive, they most probably include climatic^{10,12,13} and human¹⁴ factors, or a combination of both^{1,11,15}. However, the reduced precipitation resulting from a weakening Asian monsoon was thought to be the principal factor controlling green/sandy shifts in these areas^{6–9}.

Here we report on a Mid to Late Holocene microcharcoal record used as a proxy for fire characteristics in the Mu Us Sandy Lands (Fig. 1B) in an attempt to explore the relation between fire and RDEs. This allows us to offer some suggestions regarding the future ecological management of sandy areas in the Mu Us Sandy Lands.

Materials

The Mu Us Sandy Lands are surrounded by the Yellow River to the west, north and east, and are adjacent to the neighboring Chinese Loess Plateau (CLP) to the southeast (Fig. 1A). The region is dominated by a typical arid/semiarid continental monsoonal climate, with a mean annual temperature of 6–9°C and mean annual precipitation of 200–400 mm. Mean annual evaporation is 1800–2500 mm. In winter, the prevailing northwesterly winds near the surface play an important role in defining the most powerful sandstorm pathways (Fig. 1B). Temperate desert steppe and steppe dominate this area, dominated by *Artemisia*, *Caragana*, *Salix* and *Hippophae*.

The JJ Profile (38°44.594'N, 110°10.044'E; 1159 m above sea level) is located in the second terrace of the Tuwei River, a branch of the Yellow River, on the eastern edge of the Mu Us Sandy Lands. The profile is 740 cm deep; from the base upwards it is stratigraphically divided into paleosol, eolian sand, weakly-developed paleosol and gramineous layers (Fig. 2A). Strata at ~ 510 cm and ~ 230 cm are correlated with two RDEs (RDE-I, $\sim 4.6 \pm 0.2$ ka BP; RDE-II, $\sim 3.3 \pm 0.2$ ka BP (Fig. 2B), respectively) characterized by $\sim 100\%$ coarse sand quartz ($>63 \mu\text{m}$) (Fig. 2C).

¹Key Laboratory of Desert and Desertification, Cold and Arid Regions Environmental and Engineering Institute, Chinese Academy of Sciences, Lanzhou 730000, China. ²Northwest Institute of Historical Environment and Socio-Economic Development, Sha'anxi Normal University, Xi'an 710062, China. Correspondence and requests for materials should be addressed to Y.M. (email: miaoyunfa@lzb.ac.cn)

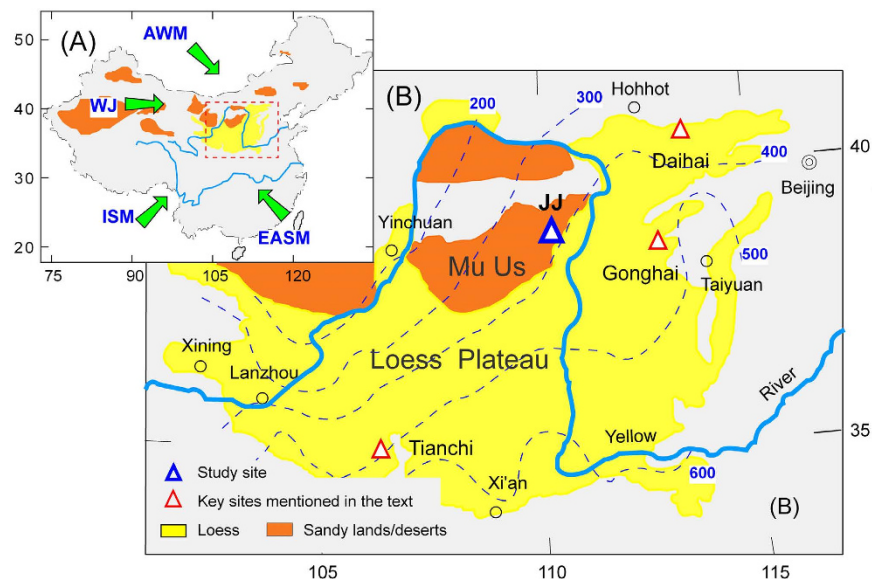


Figure 1. (A) Major atmospheric circulation regimes in East Asia and (B) the geographical location of the Mu Us Sandy Lands, including the location of the JJ Profile. Dashed lines denote mean annual precipitation isohyets. ISM: Indian Summer Monsoon; EASM: East Asian Summer Monsoon; EAWM: East Asian Winter Monsoon, WJ: Westerly jetstream. Hollow red triangles show the locations of Daihai Lake^{3,6,9}, Gonghai Lake⁷ and Tianchi Lake⁸. The map was generated by the software Adobe® FreeHand MX.

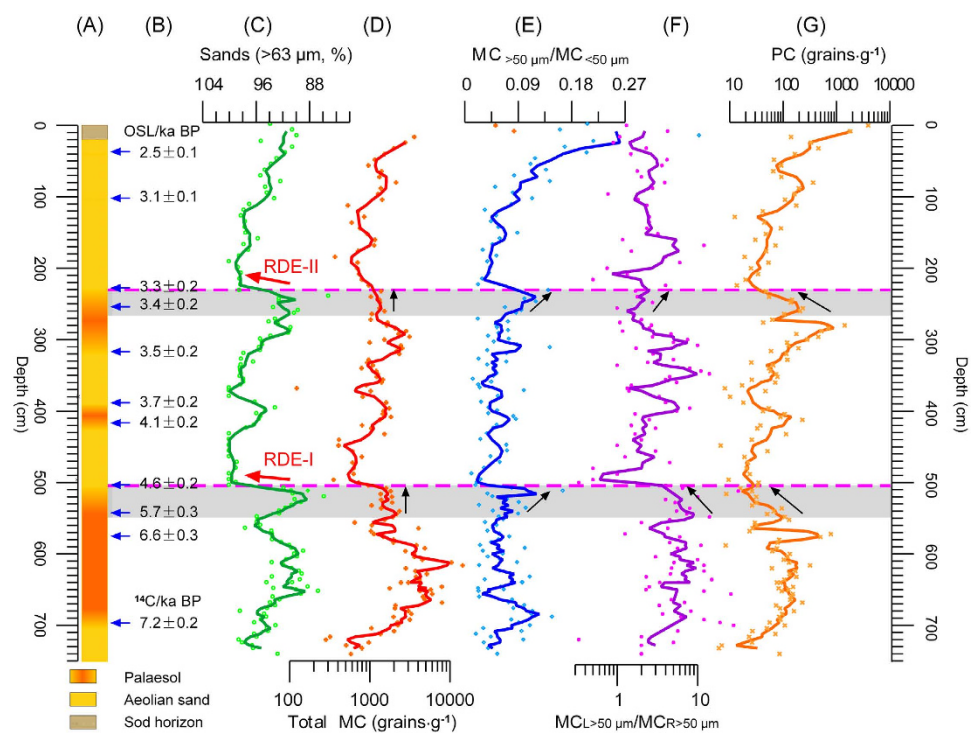


Figure 2. Comprehensive correlations in (A) lithology, (B) dating, (C) sand (>63 μm) content, (D) total MC, (E) $MC_{>50\mu m}/MC_{<50\mu m}$, (F) $CC_{>50\mu m}/CC_{<50\mu m}$ and (G) total PC in the Mu Us JJ Profile. All curves are smoothed using a 3-point running average. Gray rectangles show the two periods of abnormal fire patterns prior to the RDEs. Horizontal dotted lines show the boundaries of the RDEs. Black arrows show direction of trends. RDEs: rapid desertification events. MC: microcharcoal concentration. PC: pollen concentration.

Microcharcoals were extracted using a standard pollen methodology (SI text and Fig. S1). A known number of *Lycopodium clavatum* spores were initially added to each sample for calculating the microcharcoal concentration

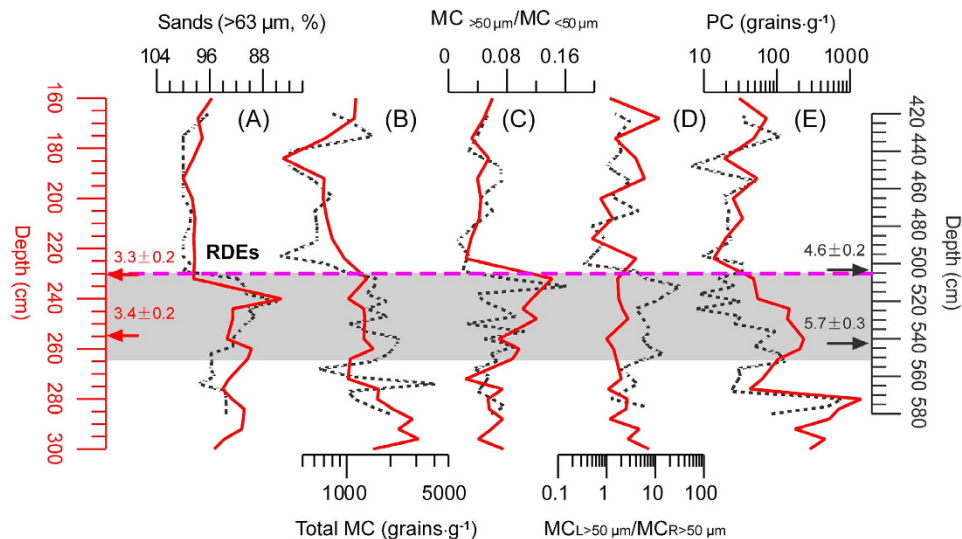


Figure 3. Comparisons between (A) sand content, (B) total MC, (C) the $MC_{>50\mu m}/MC_{<50\mu m}$ ratio, (D) the $MC_{L>50\mu m}/MC_{R>50\mu m}$ ratio and (E) PC across RDE-I (continuous red line) and RDE-II (dashed black line) in the JJ Profile, Mu Us Sandy Lands.

(MC). Additionally, four grain-size groups ($<30\mu m$, $30\text{--}50\mu m$, $50\mu m$ and $>100\mu m$), and two shape types (sub-round (R) and sub-long (L)), were identified. Here, total MC (Fig. 2D), $MC_{>50\mu m}/MC_{<50\mu m}$ (Fig. 2E) and $MC_{L>50\mu m}/MC_{R>50\mu m}$ (Fig. 2F) ratios were obtained to infer fire strength (frequency and/or intensity), fire travel distance (open and/or local) and fire material types (herbaceous and/or woody), respectively; additionally, the total pollen concentration (PC) was employed to assess vegetation coverage (Fig. 2G).

Results and Discussion

Total MC varies between ~ 30 and ~ 3200 grains $\cdot g^{-1}$, with an average of ~ 940 grains $\cdot g^{-1}$ (Fig. 2D), and maintains a roughly opposing pattern to that of the sand content (grain-size of $>63\mu m$). At the same time, the $MC_{>50\mu m}/MC_{<50\mu m}$ ratio remains at a stable value of ~ 0.07 except for in the uppermost part of the Profile (where it reaches ~ 0.27) (Fig. 2E). The $MC_{L>50\mu m}/MC_{R>50\mu m}$ ratio varies between 32.0 and 0.3, with a mean of 4.8 (Fig. 2F). The PC ranges roughly between 3912 and 6 grains $\cdot g^{-1}$, with a mean of ~ 154 grains $\cdot g^{-1}$; it follows a pattern that is roughly similar to that of total MC (Fig. 2G).

According to the assemblages, three distinct periods of fire strength versus vegetation cover are identified. Before 4.6 ± 0.2 ka BP (Stage I), the relation between fire and vegetation evinces a ‘bow’ shape pattern. Between 4.6 ± 0.2 ka BP and 3.3 ± 0.2 ka BP (Stage II), this relation exhibits a gentle, similarly increasing trend. After 3.3 ± 0.2 ka BP (Stage III), the relation between fire and vegetation follows a similar pattern to Stage II, though with a sharp increase in distances traveled by fires toward the end of the period (Fig. 2E).

Fire trends and climate change. As the residual matter from the incomplete burning of vegetation, microcharcoal is usually considered as the most reliable natural proxy for assessing the intensity and strength of fires^{16–18}. The singular wind-blown nature of the JJ Profile indicates that, here at least, total MC is indeed likely to be a good proxy for the intensity and frequency of any fires^{16,17,19–21}; the relatively larger grains tend to travel a shorter distance and reflect local fire characteristics²¹, and are associated with a high $MC_{>50\mu m}/MC_{<50\mu m}$ ratio; the sub-long and sub-round shapes of grains are linked to vegetation types, and in particular grasses and woody plants²², with a greater $MC_{L>50\mu m}/MC_{R>50\mu m}$ ratio indicating a relatively greater proportion of grasses. At the same time, a higher PC can indicate dense vegetation cover (or vegetation mass) under a moister climate, especially when located under a single wind-blown sedimentary layer^{23,24}.

During Stage I, the ‘bow’ shape of the vegetation cover versus fire strength time series correlated well with the reconstructed precipitation record based on pollen data from lakes Tianchi and Gonghai⁷, indicating a correspondingly wetter climate during the Mid Holocene. The chemical proxies (Ru/Sr, CIA *etc.*) in the JJ Profile further supported such a climatic pattern⁵. The black carbon content from Daihai Lake also experienced a ‘bow’-shaped trend, with strong fluctuations⁹, attributed to the result of the increasing vegetation cover under an improving climate, leading to more vegetation being available for combustion^{9,25}.

Fire aberrances before RDEs. When looking at the records in more detail, total MC, $MC_{>50\mu m}/MC_{<50\mu m}$, $MC_{L>50\mu m}/MC_{R>50\mu m}$ and PC before the two RDEs exhibit particular characteristics (Fig. 3): both total MC records maintain stable values between $\sim 1000\text{--}1100$ grains $\cdot g^{-1}$; the $MC_{>50\mu m}/MC_{<50\mu m}$ ratios increase obviously from ~ 0.08 to ~ 0.16 ; the $MC_{L>50\mu m}/MC_{R>50\mu m}$ ratios evince clear gaps (~ 2 in RDE-I and ~ 10 in RDE-II); and total PC decreases gradually from ~ 200 to ~ 20 grains $\cdot g^{-1}$.

A dry climate and frequent strong winds promote desertification. One classic explanation of the above results is the influence of nonlinear relations combined with feedback between desertification and the atmosphere^{12,21,26,27}.

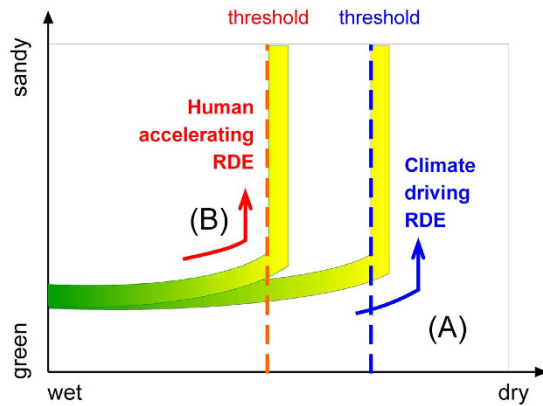


Figure 4. RDE threshold model for the Mu Us Sandy Lands based on responses to climate change and human activity indicated by fire records. (A) As precipitation decreases, the system moves towards a drier state, resulting in a crossing of the RDE threshold¹². **(B)** After superimposing human activity, under a background of decreasing precipitation, we encounter the irreversible destruction of vegetation beyond the RDE threshold, when vegetation is used for fuel.

However, the most recent results support the view that atmospheric change seem to occur contemporaneously and widely, meaning that any sediments extant under such an atmosphere can exhibit similar responses. For example, millennial-scale Younger Dryas and Heinrich events are well-recorded by coarser grain-sizes on the CLP, where such sediments were transported further, and deposited by, the stronger winds resulting from a cooler drier climate⁴. This suggests that any Holocene dry events should also be contemporaneous with changes in sedimentary characteristics under the similar atmospheric dynamics²⁸. Regardless of any nonlinear^{12,26,27} or linear relations^{6,7}, desertification in North China has tended to occur under a cool/dry climate^{1,4,10,11}.

However, through careful comparison, these two RDEs at 4.6 ± 0.2 ka BP and 3.3 ± 0.2 ka BP cannot be directly attributed to climate change, owing to the following four key contradictions. (i) These RDEs occur synchronously in the JJ Profile and at Daihai Lake³, which is difficult to dismiss as merely a coincidence. Because at Daihai Lake, RDE-II occurs during a period which is characterized by a rapid decrease in tree pollen, whereas RDE-I occurs when tree pollen percentages are high. These two RDEs cannot both therefore be explained as being the result of a climatic deterioration (cooling and drying) in the climate⁶. Additionally, at Lakes Gonghai⁷ and Tianchi⁸, the climate begins to deteriorate at 5.3 ka BP, but no obvious rapid climate change events occur during that time. (ii) Total MC and PC trends follow different directions, whereas according to the precipitation data from Stage I, they should have declined similarly along with the deterioration in the climate. (iii) The relatively local fires become consistently stronger, meaning that the area proximate to the JJ Profile experienced the burning of greater quantities of vegetation, rather than the lesser quantities of vegetation that would be expected were the climatic deteriorating. (iv) There exist sharply different fire abnormality timespans prior to these two RDEs: over 1000 years versus 100 years, and under relatively ‘better’ and ‘worse’ vegetation/climate conditions, respectively. If these RDEs were merely controlled by climate abnormality, they might exhibit similar timespans *vis-à-vis* millennial-scale oscillations^{28–31}.

Human activities driving RDEs. We therefore propose that the aberrant patterns of fire intensity/strength exhibited prior to both RDEs are the direct result of human activity, *i.e.* the excessive burning of vegetation for fuel, and an accelerating land surface degradation beyond the RDE threshold. Humans exert a definitive impact upon the environment, as when they alter terrestrial vegetation patterns during the rapid development of agriculture, and when a sharp increase in the population necessitates significant changes in land use³². This is especially marked when considerable quantities of vegetation are burnt for fuel^{33,34}. Under such a scenario, the vegetation coverage and local environment may be significantly altered by “slash and burn” agricultural activity, rural construction, and the use of fire for producing pottery, cooking and providing warmth³⁴.

The Mu Us Sandy Lands and their neighboring regions have been intensively inhabited since at least the Last Glacial Maximum³⁵. Human agriculture flourished during the Holocene, especially in cultural periods such as the Yangshao, Longshan, Zhukaigou and Maoqinggou (~ 9.0 – 2.0 ka BP)^{36–39}. Over 400 ancient cultural sites dating to before 4.0 ka BP have been identified in the Mu Us Sandy Lands⁴⁰. Additionally, several fire events appear to have occurred in the regions surrounding the Mu Us Sandy Lands, based on charcoal assemblages³⁴ and total MC^{8,21} and black carbon content⁹ values. These show multiple periods of human activity at different sites during the Mid to Late Holocene. For example, the Shimou archeological site in the Mu Us Sandy Lands, ~ 20 km to the south of the JJ Profile, has been listed in the world’s top ten ‘Ten Amazing Cities from the Ancient World’ (<http://www.ancient-origins.net>). Covering over four square kilometers, this stone city, with numerous carved jade and mural fragments, indicates the existence of a very prosperous urbanized society at ~ 4 ka BP.

Discussion and Conclusion

After considering the relations between RDEs, climate change and human activity in the Mu Us Sandy Lands, we outlined our RDE trigger models. Based simply upon the deterioration in the climate, the lands system moves towards a drier state until it reaches the RDE threshold (Fig. 4A); this can reasonably be applied to an area such as the Hunshandake Sandy Lands before groundwater extraction is taken into account¹². After superimposing human activity, under the same climatic process, the barren land surface caused by human activity can accelerate any risk that the RDE threshold is crossed (Fig. 4B). In the historic Mu Us Sandy Lands this finding is coincident with the data from many Neolithic and Bronze Age archeological sites in this region^{36,38,40} (Fig. S7).

Today, the Mu Us Sandy Lands are an important agro-pastoral transition zone and a powerful ecologically-protective screen preventing the incursion of deserts from the south and east. According to this analysis, future major ecological rehabilitation should focus on improving vegetation coverage and avoiding fire hazards to reduce the risk of desertification. Once the vegetation has been seriously damaged, land degeneration will greatly increase the risk that the RDE threshold is crossed.

References

1. Wang, X. M., Chen, F. H., Hasi, E. & Li, J. C. Desertification in China: an assessment. *Earth-Sci. Rev.* **88**, 188–206 (2008).
2. Wu, B. & Ci, L. J. Landscape change and desertification development in the Mu Us Sandland, Northern China. *J. Arid Environ.* **50**, 429–444 (2002).
3. Peng, Y. J., Xiao, J. L., Nakamura, T., Liu, B. L. & Inouchi, Y. Holocene East Asian monsoonal precipitation pattern revealed by grain-size distribution of core sediments of Daihai Lake in Inner Mongolia of north-central China. *Earth Planet. Sci. Lett.* **233**, 467–479 (2005).
4. Sun, Y. B. *et al.* Influence of Atlantic meridional overturning circulation on the East Asian winter monsoon. *Nature Geosci.* **5**, 46–49 (2011).
5. Liu, B. *et al.* Holocene moisture change revealed by the Rb/Sr ratio of aeolian deposits in the southeastern Mu Us Desert, China. *Aeolian Res.* **13**, 109–119 (2014).
6. Xiao, J. L. *et al.* Holocene vegetation variation in the Daihai Lake region of north-central China: a direct indication of the Asian monsoon climate history. *Quaternary Sci. Rev.* **23**, 1669–1679 (2004).
7. Chen, F. H. *et al.* East Asian summer monsoon precipitation variability since the last deglaciation. *Sci. Rep.* **5**, 11186 (2015).
8. Zhao, Y. *et al.* Vegetation history, climate change and human activities over the last 6200 years on the Liupan Mountains in the southwestern Loess Plateau in central China. *Palaeoogeogr. Palaeoecol.* **293**, 197–205 (2010).
9. Wang, X., Xiao, J. L., Cui, L. L. & Ding, Z. L. Holocene changes in fire frequency in the Daihai Lake region (north-central China): indications and implications for an important role of human activity. *Quaternary Sci. Rev.* **59**, 18–29 (2013).
10. Lu, H. Y. *et al.* Late Quaternary Aeolian activity in the Mu Us and Otindag dune fields (north China) and lagged response to insolation forcing. *Geophys. Res. Lett.* **32**, L21716 (2005).
11. Sun, J. M., Li, S. H., Han, P. & Chen, Y. Y. Holocene environmental changes in central Inner Mongolia, based on single-aliquot-quartz optical dating and multi-proxy study of dune sands. *Palaeoogeogr. Palaeoecol.* **233**, 51–62 (2006).
12. Yang, X. P. *et al.* Groundwater sapping as the cause of irreversible desertification of Hunshandake Sandy Lands, Inner Mongolia, northern China. *Proc. Natl. Acad. Sci. USA* **112**, 702–706 (2015).
13. Yancheva, G. *et al.* Influence of the intertropical convergence zone on the East-Asian monsoon. *Nature* **445**, 74–77 (2007).
14. Dodson, J. *et al.* Early bronze in two Holocene archaeological sites in Gansu, NW China. *Qua. Res.* **72**, 309–314 (2009).
15. Dong, G. R., Gao, S., Jin, J. & Li, B. The formation, evolution and cause of the Mu Us desert in China. *Sci. China, Ser. B.* **32**, 33–45 (1989).
16. MacDonald, G. M. *et al.* The reconstruction of boreal forest fire history from lake sediments: A comparison of charcoal, pollen, sedimentological, and geochemical indices. *Quaternary Sci. Rev.* **10**(1), 53–71 (1991).
17. Patterson, W. A., Edwards, K. J. & Maguire, D. J. Microscopic charcoal as a fossil indicator of fire. *Quaternary Sci. Rev.* **6**, 3–23 (1987).
18. Ward, D. E. & Hardy, C. C. Smoke emissions from wildland fires. *Environ. Int.* **17**, 117–134 (1991).
19. Clark, J. S. Particle motion and the theory of charcoal analysis: source area, transport, deposition and sampling. *Quaternary Res.* **30**, 67–80 (1988).
20. Sadori, L. & Giardini, M. Charcoal analysis, a method to study vegetation and climate of the Holocene: The case of Lago di Pergusa (Sicily, Italy). *Geobios* **40**, 173–180 (2007).
21. Huang, C. C. *et al.* Charcoal records of fire history in the Holocene loess-soil sequences over the southern Loess Plateau of China. *Palaeoogeogr. Palaeoecol.* **239**, 28–44 (2006).
22. Charles, E. U. & Molly, J. M. Experimental production and analysis of microscopic charcoal from wood, leaves and grasses. *Holocene* **8**, 341–346 (1998).
23. Cai, M. T. *et al.* Vegetation and climate changes during three interglacial periods represented in the Luochuan loess-paleosol section, on the Chinese Loess Plateau. *Quatern. Int.* **296**, 131–140 (2013).
24. Liu, K. B., Yao, Z. J. & Thompson, L. A pollen record of Holocene climatic changes from Dundee ice cap, Qinghai-Tibetan Plateau. *Geology* **26**, 135 (1998).
25. Whitlock, C. & Larsen, C. Charcoal as a fire proxy. *Develop. Paleoenviron. Res.* **3**, 75–97 (2002).
26. Scheffer, M., Carpenter, S., Foley, J. A., Folke, C. & Walker, B. Catastrophic shifts in ecosystems. *Nature* **413**, 591–596 (2001).
27. Claussen, M. *et al.* Simulation of an abrupt change in Saharan vegetation in the mid-Holocene. *Geophys. Res. Lett.* **26**, 2037–2040 (1999).
28. Bond, G. *et al.* A pervasive millennial-scale cycle in North Atlantic Holocene and glacial climates. *Science* **294**, 2130–2136 (2001).
29. Bianchi, G. G. & McCave, I. N. Holocene periodicity in North Atlantic climate and deep-ocean flow south of Iceland. *Nature* **397**, 513–515 (1999).
30. David, J. R., Thornalley, H. E. & McCave, I. N. Holocene oscillations in temperature and salinity of the surface subpolar North Atlantic. *Nature* **457**, 711–714 (2009).
31. Matt, S. M. *et al.* Divergent trends in land and ocean temperature in the Southern Ocean over the past 18000. *Nature* **931**, 622–626 (2010).
32. Vitousek, P. M., Mooney, H. A., Lubchenco, J. & Melillo, J. M. Human domination of Earth's ecosystems. *Science* **277**, 494–99 (1997).
33. Prins, F. & Shackleton, C. M. Charcoal analysis and the “Principle of Least Effort”-A conceptual Model. *J. Archaeol. Sci.* **19**, 631–637 (1992).
34. Li, X. Q., Sun, N., Dodson, J. & Zhou, X. Y. Human activity and its impact on the landscape at the Xishanping site in the western Loess Plateau during 4800–4300 cal yr BP based on the fossil charcoal record. *J. Archaeol. Sci.* **39**, 3141–3147 (2012).
35. Liu, L., Bestel, S., Shi, J., Song, Y. & Chen, X. Paleolithic human exploitation of plant foods during the last glacial maximum in North China. *Proc. Natl. Acad. Sci. USA* **110**, 5380–5385 (2013).
36. Inner Mongolia Culture and Archaeology Institute, *Proceedings of Researches on the Primitive Culture in Central-Southern Inner Mongolia* (China Ocean Press, Beijing, 1991).

37. Lian, P. L. & Fang, X. Q. On the relationship between the development of prehistorical cultures and environmental change in the Daihai Lake Region, Inner Mongolia. *Dili Yanjiu (Geographical Research)* **20**, 623–628 (2001).
38. State Administration of Cultural Heritage, *Atlas of Chinese cultural relics, Shaanxi* (Xi'an Cartographic Publishing House, Xi'an, 1998).
39. Wagner, M. *et al.* Mapping of the spatial and temporal distribution of archaeological sites of northern China during the Neolithic and Bronze Age. *Quatern. Int.* **290–291**, 344–357 (2013).
40. Zhuo, H. X., Lu, H. Y., Jia, X. & Sun, Y. G. A preliminary study on human activities in sand fields of northern China and its relationship with the climatic variations in Holocene. *Disiji Yanjiu (Quaternary Sciences)*, **33(2)**, 303–313 (2013).

Acknowledgements

We are grateful to the helpful Y.D., Duan, Y.Y., Zhao, Y.H., Miao, and F.Z., Zhang for assistance in laboratory and field help. This research was funded by the Knowledge Innovation Program of the Chinese Academy of Sciences (Grant No. KZZD-04-04), the National Natural Science Foundation of China (Grant Nos. 41172153, 41271215). The materials used in this paper are housed in the Key Laboratory of Desert and Desertification, Cold and Arid Regions Environmental and Engineering Institute, Chinese Academy of Sciences. Data are available in the supplementary materials.

Author Contributions

Y.F.M. and H.L.J. designed the study and wrote the manuscript. Y.F.M. and J.X.C. analysed the data and reviewed the manuscript.

Additional Information

Supplementary information accompanies this paper at <http://www.nature.com/srep>

Competing financial interests: The authors declare no competing financial interests.

How to cite this article: Miao, Y. *et al.* Human activity accelerating the rapid desertification of the Mu Us Sandy Lands, North China. *Sci. Rep.* **6**, 23003; doi: 10.1038/srep23003 (2016).



This work is licensed under a Creative Commons Attribution 4.0 International License. The images or other third party material in this article are included in the article's Creative Commons license, unless indicated otherwise in the credit line; if the material is not included under the Creative Commons license, users will need to obtain permission from the license holder to reproduce the material. To view a copy of this license, visit <http://creativecommons.org/licenses/by/4.0/>